Supplementary Material for "**Zonation of hepatic fat accumulation: Insights from mathematical modelling of nutrient gradients and fatty acid uptake**"

Jana Schleicher[1,2]*, Uta Dahmen[1], Reinhard Guthke[3], Stefan Schuster[2]

[1] Experimental Transplantation Surgery, Department of General, Visceral and Vascular Surgery, University Hospital Jena, Germany

[2] Department of Bioinformatics, Friedrich-Schiller-University Jena, Germany

[3] Leibniz Institute for Natural Product Research and Infection Biology - Hans Knoell Institute, Germany

Published by *Journal of the Royal Society Interface* 2017.

**Supplementary Content:**

**<u>Supplement S1</u> Detailed description of the metabolic model versions**

*A constitutive metabolic model without nutrient blood gradients (model version 1)*

In a first step, a minimal model of hepatic fatty acid (FA) metabolism was developed. The consideration of FA metabolism was restricted to one compartment representing one hepatic zone along the sinusoid (n=1). Our model comprises the following metabolic pathways: FA uptake from the blood, mitochondrial FA oxidation, triglycerides (TG) synthesis, TG secretion, uptake of oxygen ($O_2$) from the blood and use of $O_2$ by processes other than mitochondrial FA oxidation (e.g. for glucose oxidation). The time unit is minutes.

This model version was used to find suitable parameter values (see *Supplement S4* "*Model parameter calibration"*) and to evaluate parameters with regard to their importance in determining the accumulation of TGs independent of metabolite gradients (sensitivity analysis). Moreover, with this basic model, we can examine the fundamental effect of FA uptake kinetics (linear versus nonlinear) on TG accumulation.

To simulate the supply of FAs and $O_2$ by sinusoidal blood flow within the liver, we estimated blood values of FA and $O_2$ concentrations from the literature. The amount of blood flowing per minute through the human liver is 1500 ml/min [1]. Commonly reported FA concentrations in human plasma ranges between 0.1 µmol/$ml_{blood}$ and 1.4 µmol/$ml_{blood}$ [2-4]; this range is used in our model for the simulation under a low and a high FA supply, respectively. In our model, we do not differentiate among different types of FA species. Generally, FA inflow in the blood compartment was calculated in the following way for a low (Eq. 1a) and a high fat diet (Eq. 1b):

$$v_{FA\_inflow} = 1500\,\frac{ml_{blood}}{min} * 0.1\,\frac{\mu mol}{ml_{blood}} = 150\,\frac{\mu mol}{min} \qquad \text{(Eq. 1a)}$$

$$v_{FA\_inflow} = 1500\,\frac{ml_{blood}}{min} * 1.4\,\frac{\mu mol}{ml_{blood}} = 2100\,\frac{\mu mol}{min} \qquad \text{(Eq. 1b)}$$

To estimate blood $O_2$ supply, we only considered the concentration of bound oxygen and neglected the concentration of free $O_2$ in the blood due to its very low concentration. The periportal

oxygen concentration is 84-91 µmol/$l_{blood}$ (60 – 65 mmHG) [5] and the (maximal) oxygen blood flow (Eq. 2; in µmol/min) in our model is therefore calculated similar to the FA blood supply above:

$$v_{O2\_inflow} = 1500\frac{ml_{blood}}{min} * 0.091\frac{\mu mol}{ml_{blood}} = 136.5\frac{\mu mol}{min} \quad \text{(Eq. 2).}$$

The rate of FA uptake (in µmol/min) can be simulated either as a linear, nonsaturable process [6, 7] (Eq. 3) or as a saturable process using Michaelis-Menten kinetics [8-11] (Eq. 4). Parameter values of FA uptake ($k_{FAup}$, $v_{max\_FAup}$, $K_{M\_FAup}$) were chosen to lead to nearly similar uptake rates under a low FA blood concentration in the linear and nonlinear model. We chose a $K_{M\_FAup}$ of 300 µM for the nonlinear uptake kinetics, thus matching the basal range of total plasma FA concentration in healthy humans (100 to 400 µM [12]).

$$v_{FA\_uptake} = k_{FAup} * [FA]_{blood} \quad \text{(Eq. 3)}$$

$$v_{FA\_uptake} = \frac{v_{\max\_FAup} * [FA]_{blood}}{K_{M\_FAup} + [FA]_{blood}} \quad \text{(Eq. 4)}$$

The rate of $O_2$ uptake (in µmol/min) from the blood into hepatocytes is simulated using Michaelis-Menten kinetics [13] (Eq. 5).

$$v_{O2\_uptake} = \frac{v_{\max\_O2up} * [O2]_{blood}}{K_{M\_o2up} + [O2]_{blood}} \quad \text{(Eq. 5)}$$

The use of $O_2$ for other oxidative processes, such as glucose oxidation, is factored in by implementing a degradation rate for $O_2$ (mass action law; Eq. 6; in µmol/min). This prevents a continuous increase of the $O_2$ concentration within the compartment under low FA concentration and allows the establishment of a steady state.

$$v_{O2\_degr} = k_{degrad\_o2} * \left[O2_{comp}\right]_{n=1} \text{ (Eq. 6)}$$

The rate of mitochondrial FA oxidation (Eq. 7; in µmol/min) depends on the FA and $O_2$ concentrations within the hepatic compartment (n=1). The amount of oxygen limits this process.

$$v_{oxidation} = \frac{k_{oxid} * [FA_{comp}]_{n=1} * [O2_{comp}]_{n=1}}{K_{oxid} + [O2_{comp}]_{n=1}} \qquad \text{(Eq. 7)}$$

The synthesis of TGs (Eq. 8; in µmol/min) is implemented with a reversible mass action law to account for the lipolysis/re-esterification cycle of TGs [14]:

$$v_{TG\_syn} = k_{for\_TGsyn} * [FA_{comp}]_{n=1} - k_{back\_TGsyn} * [TG_{comp}]_{n=1} \qquad \text{(Eq. 8)}$$

The export of TGs (Eq. 9; in µmol/min) depends on the concentration of TGs and not on the concentration of FAs [15]. Thus, the export flux is calculated in the following way:

$$v_{TG\_export} = k_{ex\_TG} * [TG_{comp}]_{n=1} \qquad \text{(Eq. 9)}$$

Therefore, considering the concentrations of FAs, $O_2$ and TGs in a hepatic compartment, a system of three ODEs is implemented in model version 1:

$$\frac{d[FA_{comp}]_{n=1}}{dt} = v_{FA\_uptake} - v_{TG\_syn} - v_{oxidation} \qquad \text{(Eq. 10a)}$$

$$\frac{d[O2_{comp}]_{n=1}}{dt} = v_{O2\_uptake} - v_{oxidation} - v_{O2\_degr} \qquad \text{(Eq. 10b)}$$

$$\frac{d[TG_{comp}]_{n}}{dt} = v_{TG\_syn} - v_{TGexport} \qquad \text{(Eq. 10c)}$$

*Zonated metabolic models with nutrient blood gradients (model versions 2 – 4)*

Model 1 was extended by implementing three metabolic compartments (n = 1, 2, 3) consecutively, each with the metabolic pathways described above. Each metabolic compartment represents one of the three zones along a sinusoid (i.e. periportal zone n=1, middle zone n=2, and pericentral zone n= 3) [16]. The three compartments are assumed to be distributed almost similar along a blood vessel and the total cell volume of each zone can be roughly approximated to be one-third [17]. Reactions and parameter values are similar in each of the three compartments; preventing *a prior* establishment of a zonation pattern due to differences in parameter values. In addition to the three metabolic compartments, we established a fourth compartment representing the hepatic blood vessel. Here the initial concentrations of FAs and $O_2$ in periportal blood are used as input (see above, Eq. 1a, b and Eq. 2). The blood compartment allows an establishment of gradients of FAs and $O_2$ from the periportal to the pericentral compartment. This was done by using a flow constant ($k_{flow}$) for the "transport" of metabolites (FAs and oxygen) in the blood compartment.

Each of the three metabolic compartments (n=1, 2, 3) takes up FAs and $O_2$ from the associated blood FA and $O_2$ values and, therefore, decreases the concentrations for the subsequent compartment(s) (see Fig. 1 in the *manuscript*). This is in accordance to the observation that the first (periportal) hepatocytes influence the concentration of substances for pericentral hepatocytes by their uptake and release activities. The flow of substrates (i.e. FAs and $O_2$, Eq. 11) within the blood compartment was modelled according to mass action kinetics:

$$rate_{flow\ n\ ->\ n+1} = k_{flow} * [substrate]_n \qquad \text{(Eq. 11)}$$

As presented in Table 1 and Fig. 1 in the *manuscript*, model version 2 was implemented only with an oxygen gradient. Model version 3 was implemented with a FA gradient, whereas model version 4, finally, incorporates both gradients. Each model version was simulated with a linear and a nonlinear FA uptake kinetics, respectively (see above Eq. 3 and Eq. 4).

Model version 2 consists of the following ordinary differential equations in each metabolic compartment (n = 1, 2, 3). The values of $[FA]_{blood\_n}$ is similar for n=1…3.

$$rate_{O2\_flow\ n->n+1} = k_{flow} * [O2]_{blood\_n} \quad \text{(Eq. 12a)}$$

$$\frac{d[FA_{comp}]_n}{dt} = k_{FAup} * [FA]_{blood\_n} - k_{for\_TGsyn} * [FA_{comp}]_n + k_{back\_TGsyn} * [TG_{comp}]_n - \frac{k_{oxid} * [FA_{comp}]_n * [O2_{comp}]_n}{K_{oxid} + [O2_{comp}]_n} \quad \text{(Eq. 12b)}$$

$$\frac{d[O2_{comp}]_n}{dt} = \frac{v_{\max\_O2up} * [O2]_{blood\_n}}{K_{M\_O2up} + [O2]_{blood\_n}} - k_{degrad\_O2} * [O2_{comp}]_n - \frac{k_{oxid} * [FA_{comp}]_n * [O2_{comp}]_n}{K_{oxid} + [O2_{comp}]_n} \quad \text{(Eq. 12c)}$$

$$\frac{d[TG_{comp}]_n}{dt} = k_{for\_TGsyn} * [FA_{comp}]_n - k_{back\_TGsyn} * [TG_{comp}]_n - k_{ex\_TG} * [TG_{comp}]_n \quad \text{(Eq. 12d)}$$

In model version 3, the simulation under a FA blood gradient was conducted, whereas the blood O2 concentration ($[O2]_{blood\_n}$) is similar for each metabolic compartment. The system of ODEs is similar to model version 2 (Eq. 12b-d) with additional Eq. 13 (instead of Eq. 12a).

$$rate_{FA\_flow\ n->n+1} = k_{flow} * [FA]_{blood\_n} \quad \text{(Eq. 13)}$$

In model version 4, we combined the metabolic gradients of FAs and oxygen (Eqs. 12a-d, 13). The model codes (in R) can be provided upon request from the corresponding author.

**Supplement S2** Sensitivity analysis of model version 4, hepatic fatty acid (FA) metabolism with declining FA and oxygen gradients from periportal to pericentral. The model was implemented with a linear FA uptake. Dimensionless sensitivity functions are shown for running the model under a low FA and a high FA supply via blood. For each model run, only the 4 most influential parameters are plotted due to facility of inspection. Under low FA supply the flow constant of metabolites ($k_{flow}$) has a high impact on the third (pericentral) compartment, because it determines how much FAs and oxygen arrives at this compartment. FA concentration in the blood ($[FA]_{blood}$) is the most relevant factor for all three compartments, as expected. Furthermore, a high impact on TG accumulation is shown by the TG synthesis parameter ($k_{for\_TGsyn}$) under a low FA supply and the export rate of TGs ($k_{ex\_TG}$) under a high FA supply via blood.

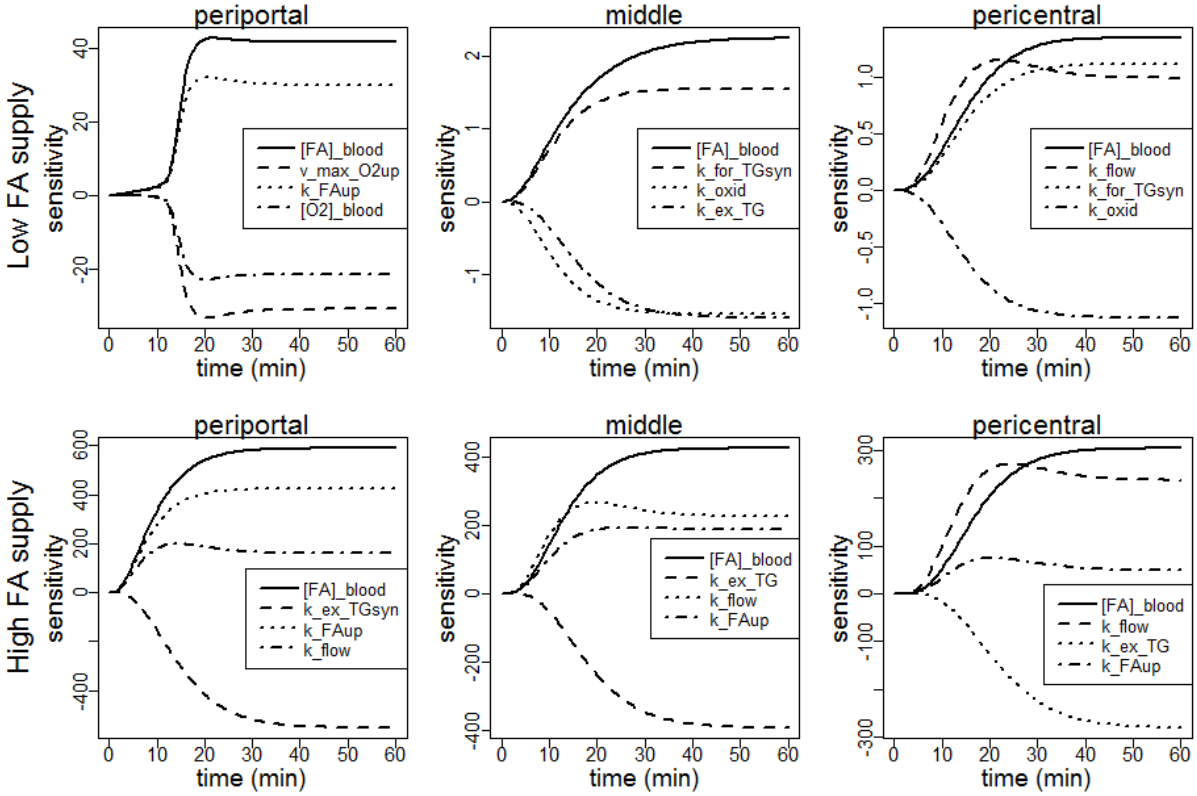

**Supplement S3** Parameter scan for different $k_{ex\_TG}$ values for the whole range of $[FA]_{blood}$ values. Simulations are shown for model version 4, hepatic fatty acid (FA) metabolism with declining FA and oxygen gradients, with nonlinear FA uptake kinetics. Blood flows from the periportal compartment (C1, solid line) to the middle (C2, dashed line) to the pericentral compartment (C3, pointed line). The export of TGs influence the amount of stored TGs in the compartments, but does not influence the pattern of zonation.

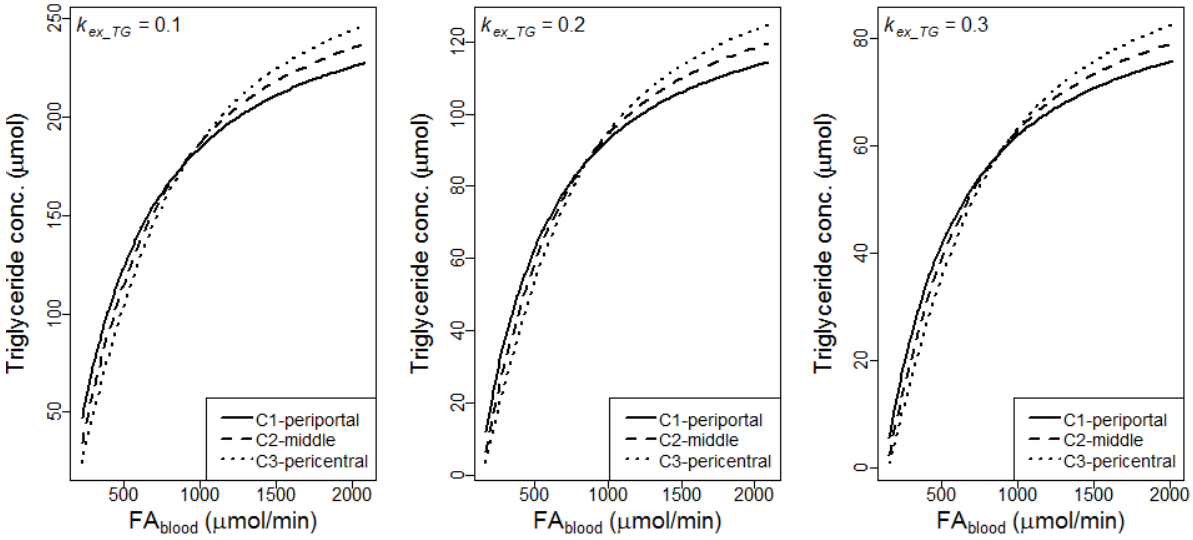

**Supplement S4 Model parameter calibration**

Parameter values and a description of each parameter are provided in Table 2 in the *manuscript*. The model represents a qualitative rather than a quantitative representation of a zonated TG accumulation along a hepatic blood vessel. This should be adequate to encourage our goal of unveiling the role of metabolic gradients and FA uptake kinetics on the direction of the zonation pattern (i.e. periportal versus pericentral fat accumulation). The model can be adapted and made more quantitative as soon as more experimental data are available.

We extracted parameter values for fatty acid and oxygen concentrations from literature (see above); however most of the kinetic parameters for FA metabolism within each hepatic zone are not available yet. Thus, the parameter values in model version 1 were adjusted until a good agreement of model output with well-known observations has been achieved. We used the following four observed physiological patterns to adjust parameter values:

(1) FA concentration in blood decreases from periportal to pericentral by ~ 50% under a low FA supply via blood [18],

(2) $O_2$ concentration in blood declines from periportal to pericentral by ~ 50% [19],

(3) increased hepatic FA inflow via blood raises TG accumulation [20], and

(4) the oxidation rate is higher than the export rate [21].

Calibration of the model with nonlinear FA uptake kinetics was conducted similar to the model with linear FA uptake. Simulation runs of the one-compartment model (model version 1) under a low FA supply via blood revealed that, as intended, TG accumulation and metabolic rates are almost similar between the linear and the nonlinear model. Under a high-fat diet, TG accumulation in the nonlinear model was lower than in the linear model (data not shown). The oxidation rate was similar between the linear and the nonlinear model implementation (due to similar oxygen supply via blood), whereas the rates of TG synthesis and TG export were greater in the linear model because of the higher uptake of FAs. Sensitivity analysis was performed for the linear and the nonlinear model version to access the most important parameters. The results are provided in the *manuscript section "Results"* and in Fig. 2.

**Supplementary References**

[1] Chalhoub E, Xie L, Balasubramanian V, Kim J, Belovich J. 2007 A distributed model of carbohydrate transport and metabolism in the liver during rest and high-intensity exercise. *Ann Biomed Eng* **35**, 474-491. (doi:10.1007/s10439-006-9217-2)

[2] Brodersen R, Andersen S, Vorum H, Nielsen SU, Pedersen AO. 1990 Multiple fatty acid binding to albumin in human blood plasma. *European Journal of Biochemistry / FEBS* **189**, 343-349.

[3] Potter BJ, Sorrentino D, Berk PD. 1989 Mechanisms of cellular uptake of free fatty acids. *Annu Rev Nutr* **9**, 253-270. (doi:10.1146/annurev.nu.09.070189.001345)

[4] Huber AH, Kleinfeld AM. 2017 Unbound free fatty acid profiles in human plasma and the unexpected absence of unbound palmitoleate. *J Lipid Res* **58**, 578-585. (doi:10.1194/jlr.M074260)

[5] Kietzmann T, Dimova EY, Flügel D, Scharf JG. 2006 Oxygen: modulator of physiological and pathophysiological processes in the liver. *Zeitschrift fuer Gastroenterologie* **44**, 67-76. (doi:10.1055/s-2005-858987)

[6] Hamilton JA, Johnson RA, Corkey B, Kamp F. 2001 Fatty acid transport: the diffusion mechanism in model and biological membranes. *J Mol Neurosci* **16**, 99-108. (doi:10.1385/JMN:16:2-3:99)

[7] Hamilton JA, Guo W, Kamp F. 2002 Mechanism of cellular uptake of long-chain fatty acids: Do we need cellular proteins? *Mol Cell Biochem* **239**, 17-23.

[8] Stremmel W, Berk PD. 1986 Hepatocellular influx of 14Coleate reflects membrane transport rather than intracellular metabolism or binding. *Proc Natl Acad Sci U S A* **83**, 3086-3090.

[9] Stremmel W, Theilmann L. 1986 Selective inhibition of long-chain fatty acid uptake in short-term cultured rat hepatocytes by an antibody to the rat liver plasma membrane fatty acid-binding protein. *Biochim Biophys Acta* **877**, 191-197.

[10] Stremmel W, Gunnawan J. 1998 Indication for a specific interaction of fatty acids with a liver sinusoidal plasma membrane carrier. *Eur J Med Res* **3**, 71-76.

[11] Sorrentino D, Stump DD, Van Ness K, Simard A, Schwab AJ, Zhou SL, Goresky CA, Berk PD. 1996 Oleate uptake by isolated hepatocytes and the perfused rat liver is competitively inhibited by palmitate. *Am J Physiol* **270**, G385-392.

[12] Glatz JF, Luiken JJ, Bonen A. 2010 Membrane fatty acid transporters as regulators of lipid metabolism: implications for metabolic disease. *Physiol Rev* **90**, 367-417. (doi:10.1152/physrev.00003.2009)

[13] Cho CH, Park J, Nagrath D, Tilles AW, Berthiaume F, Toner M, Yarmush ML. 2007 Oxygen uptake rates and liver-specific functions of hepatocyte and 3T3 fibroblast co-cultures. *Biotechnology and Bioengineering* **97**, 188-199. (doi:10.1002/bit.21225)

[14] Wiggins D, Gibbons GF. 1992 The lipolysis/esterification cycle of hepatic triacylglycerol. Its role in the secretion of very-low-density lipoprotein and its response to hormones and sulphonylureas. *Biochem J* **284 (Pt 2)**, 457-462.

[15] Gibbons GF, Bartlett SM, Sparks CE, Sparks JD. 1992 Extracellular fatty acids are not utilized directly for the synthesis of very-low-density lipoprotein in primary cultures of rat hepatocytes. *Biochem J* **287 (Pt 3)**, 749-753.

[16] Halpern KB, Shenhav R, Matcovitch-Natan O, Toth B, Lemze D, Golan M, Massasa EE, Baydatch S, Landen S, Moor AE *et al.* 2017 Single-cell spatial reconstruction reveals global division of labour in the mammalian liver. *Nature* **542**, 352-356. (doi:10.1038/nature21065)

[17] Davidson AJ, Ellis MJ, Chaudhuri JB. 2012 A theoretical approach to zonation in a bioartificial liver. *Biotechnol Bioeng* **109**, 234-243. (doi:10.1002/bit.23279)

[18] Rémésy C, Demigné C. 1983 Changes in availability of glucogenic and ketogenic substrates and liver metabolism in fed or starved rats. *Ann Nutr Metab* **27**, 57-70.

[19] Jungermann K, Kietzmann T. 2000 Oxygen: modulator of metabolic zonation and disease of the liver. *Hepatology (Baltimore, Md.)* **31**, 255-260. (doi:10.1002/hep.510310201)

[20] Donnelly KL, Smith CI, Schwarzenberg SJ, Jessurun J, Boldt MD, Parks EJ. 2005 Sources of fatty acids stored in liver and secreted via lipoproteins in patients with nonalcoholic fatty liver disease. *J Clin Invest* **115**, 1343-1351. (doi:10.1172/JCI23621)

[21] Gebhardt R. 1992 Metabolic zonation of the liver: regulation and implications for liver function. *Pharmacol Ther* **53**, 275-354.